13C NMR studies of hydrocarbon guests in synthetic Structure H gas hydrates: experiment and computation

Lee, Jong-Won; Lu, Hailong; Moudrakovski, Igor L.; Ratcliffe, Christopher I.; Ohmura, Ryo; Alavi, Saman; Ripmeester, John A.

Publisher's version / Version de l'éditeur:
http://dx.doi.org/10.1021/jp1118184
The Journal of Physical Chemistry A, 115, 9, pp. 1650-1657, 2011-02-17

THE JOURNAL OF PHYSICAL CHEMISTRY A

ARTICLE

pubs.acs.org/JPCA

^{13}C NMR Studies of Hydrocarbon Guests in Synthetic Structure H Gas Hydrates: Experiment and Computation

Jong-Won Lee,[†] Hailong Lu,[‡] Igor L. Moudrakovski,[‡] Christopher I. Ratcliffe,[‡] Ryo Ohmura,[§] Saman Alavi,[‡] and John A. Ripmeester*[,‡]

[†]Department of Environmental Engineering, Kongju National University, 275 Budae-dong, Cheonan-si, Chungnam, 331-717, Republic of Korea

[‡]Steacie Institute for Molecular Sciences, National Research Council Canada, 100 Sessux Drive, Ottawa, Ontario, K1A 0R6, Canada

[§]Department of Mechanical Engineering, Keio University, 3-14-1 Hiyoshi, Kohoku-ku, Yokohama, 223-8522, Japan

Supporting Information

ABSTRACT: ^{13}C NMR chemical shifts were measured for pure (neat) liquids and synthetic binary hydrate samples (with methane help gas) for 2-methylbutane, 2,2-dimethylbutane, 2,3-dimethylbutane, 2-methylpentane, 3-methylpentane, methylcyclopentane, and methylcyclohexane and ternary structure H (sH) clathrate hydrates of *n*-pentane and *n*-hexane with methane and 2,2-dimethylbutane, all of which form sH hydrates. The ^{13}C chemical shifts of the guest atoms in the hydrate are different from those in the free form, with some carbon atoms shifting specifically upfield. Such changes can be attributed to conformational changes upon fitting the large guest molecules in hydrate cages and/or interactions between the guests and the water molecules of the hydrate cages. In addition, powder X-ray diffraction measurements revealed that for the hexagonal unit cell, the lattice parameter along the *a*-axis changes with guest hydrate former molecule size and shape (in the range of 0.1 Å) but a much smaller change in the *c*-axis (in the range of 0.01 Å) is observed. The ^{13}C NMR chemical shifts for the pure hydrocarbons and all conformers were calculated using the gauge invariant atomic orbital method at the MP2/6-311+G(*2d,p*) level of theory to quantify the variation of the chemical shifts with the dihedral angles of the guest molecules. Calculated and measured chemical shifts are compared to determine the relative contribution of changes in the conformation and guest−water interactions to the change in chemical shift of the guest upon clathrate hydrate formation. Understanding factors that affect experimental chemical shifts for the enclathrated hydrocarbons will help in assigning spectra for complex hydrates recovered from natural sites.

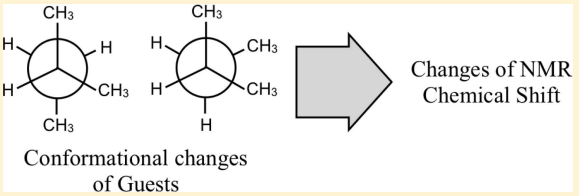

INTRODUCTION

Gas hydrates, formed by reactions of low-molecular weight hydrocarbon guests with water molecules, were identified as hazardous materials because they may cause plugging in natural gas pipelines, which may lead to damage.[1] Accordingly, researchers investigated the stability conditions of hydrates and methods of inhibiting hydrate formation in order to transport natural gas safely through pipelines without blockage.[2−4] Additionally, since huge reserves of natural gas are known to be stored naturally in the form of gas hydrates, tremendous scientific and engineering effort is being dedicated to developing natural gas hydrates as a new energy source. Hydrocarbon gas hydrates have three distinct structures, namely structure I (sI), structure II (sII), and structure H (sH). In spite of the structural differences, gas hydrates of all types can store large amounts of gas in terms of the volume ratio of gas to hydrate. They may therefore have many potential applications, for example, to separate carbon dioxide from flue gas, to sequester carbon dioxide in geologic formations in the form of gas hydrate,[5,6] or to transport and store natural gas in the hydrate form.[7]

The knowledge of both molecular (i.e., cage occupancy, hydration number) and macroscopic (i.e., temperature or pressure) properties is important for studying problems related to hydrate applications. For the molecular-scale characterization of gas hydrates, a variety of techniques, including solid-state nuclear magnetic resonance (NMR), Raman spectroscopy,[8] powder X-ray diffraction (XRD), and neutron diffraction,[9] are used, each of which has its own advantages and limitations. In case of NMR methods, the first measurement of cage occupancies was that using ^{129}Xe NMR to study xenon-containing sI and sII hydrates.[10] The first application to hydrocarbon hydrates was that of Ripmeester and Ratcliffe[11] who reported cage occupancies from ^{13}C NMR and its relation to the hydrate structure for CH_4 in sI and sII hydrates. Since then, the technique has been adopted in many research projects and has become one of the most powerful qualitative and quantitative methods for hydrate characterization.[12,13] When changing the nuclear probe used in the NMR measurements, such characterization can be expanded to a variety of guest species.[14] A general trend observed was that the isotropic

Received: December 13, 2010
Revised: January 9, 2011
Published: February 17, 2011

chemical shift scales with cage size, with guests in the smallest cages showing the largest shift difference from the gas phase because of deshielding by collisions of the guest with the cage wall.[15] In addition, it has been reported that such NMR techniques can be used to observe and analyze molecular behaviors during hydrate formation,[16] or to find new guest behaviors for sH hydrate.[17] In addition to the characterization of synthetic hydrate samples, the NMR technique can also be used for natural gas hydrate samples in order to elucidate their molecular-scale properties such as structure, composition, and relative amounts of guest species stored.[18] Recently, Lu et al.[19] investigated a natural hydrate sample taken from the Cascadia margin using various characterization techniques, including NMR, to find that it is a mixed sII and sH hydrate with a variety of heavier hydrocarbons ($>C_4$).

As such, NMR analysis is important for studying physical and structural properties of gas hydrates. Because of the larger cage sizes available in the sH hydrate, many more hydrocarbons can be guests for sH than for sI or sII hydrate, and many of these larger molecules have various degrees of conformational freedom. Thus, depending on the conformation of the guest in the cage as compared to that in the bulk pure phase, ^{13}C chemical shifts may also provide information on this molecular aspect of the guest. The bulk−cage chemical shift difference likely also has contributions from cage size effects, as described above. Thus it is valuable to have a systematic study of ^{13}C chemical shifts of more complex sH guest molecules, to note chemical shift differences between the encaged guests and the bulk and to try and explain the differences in terms of the two effects noted above. In this work, the ^{13}C NMR spectra of the hydrate samples obtained are compared with those of the hydrocarbons in the bulk. Structures of the hydrates were confirmed by powder XRD measurements and the unit cell parameters were determined. The ^{13}C chemical shifts were then calculated for different conformers of the guest molecules in order to assess the importance of conformational changes for the observed chemical shift differences.

EXPERIMENTAL AND COMPUTATIONAL METHODS

All hydrocarbon liquids were purchased from Sigma Aldrich with minimum purity of 99 mol % and were used without further treatment. The methane was UHP grade from Praxair. The hydrate samples were prepared in the same way as in our previous work.[17] First, 5.0 g of ice was ground into fine powder and loaded into a high-pressure cell before adding 1.0 mL of the hydrate formers. For hydrate samples containing *n*-pentane and *n*-hexane, a liquid mixture of 2,2-dimethylbutane (1.0 mL) and *n*-pentane or *n*-hexane (0.5 mL) were added to the prepared ice powder. To prevent the ice powder from melting or the hydrocarbons from evaporating, both the high-pressure cell and the hydrate formers were cooled in a freezer at 253.2 K before use. After loading, the high-pressure cell was moved to a water bath, cooled to a constant temperature of 271.2 K, then, CH_4 helper gas was slowly introduced to a pressure up to 30.0 bar so as not to form pure CH_4 hydrate (sI) due to the reaction between ice and CH_4 gas. When the pressure drop due to hydrate formation was observed after 1 day, the temperature was increased to 274.2 K to promote the conversion of water into hydrate. To convert additional water into hydrate, this thermal cycling was used twice. After the pressure drop reached a steady state, the cell was cooled with liquid nitrogen before releasing pressure and taking out the samples.

Structural identification of the prepared samples was carried out on a Rigaku powder X-ray diffractometer equipped with an Anton Paar low-temperature controller. This apparatus has a maximum capacity of 12 kW and can be operated down to 83.0 K. CoKα radiation (wavelength of 1.79021 Å) was used and reflections were collected from 5.0 to 50.0° with a step size of 0.05° and a step time of 5 s. During the diffraction measurements, the experimental temperature was kept at about 85.0 K with liquid nitrogen.

For compositional investigations, ^{13}C NMR spectra were obtained at 200.0 K by packing the hydrate samples in a 7-mm diameter Zirconium rotor, which was loaded into the variable temperature (VT) probe of a Bruker DSX400 solid-state NMR spectrometer. All spectra were recorded at a Larmor frequency of 100.6 MHz with magic angle spinning (MAS) at 2.0 kHz with cross-polarization (CP) or from single-pulse free induction decays with ^1H decoupling. The ^{13}C NMR resonance peaks of adamantane, with assigned chemical shifts of $\delta = 38.56$ and 29.50 ppm at 298 K, were used as the external chemical shift reference.

The ^{13}C chemical shielding of the carbon atoms for guest molecules were calculated using the gauge invariant atomic orbital (GIAO) method[20] in the Gaussian 98 suite of programs.[21] Optimized structures of each molecule at the lowest potential energy minimum and selected conformers with different dihedral angles with respect to the carbon backbones were determined with density functional theory at the B3LYP/6-311++G(*d*,*p*) level. For each optimized structure, ^{13}C NMR isotropic chemical shielding was calculated at the MP2/6-311+G(2*d*,*p*). Chemical shifts were calculated after determining the isotropic chemical shielding of tetra-methylsilane (TMS) with an identical protocol. For guest molecules with a maximum four carbon chains (i.e., 2-methybutane, 2,2-dimethylbutane, and 2,3-dimethylbutane), we have performed relaxed potential energy surface scans at 10° intervals and performed GIAO calculations to determine the chemical shifts of the carbons at each dihedral angle.

RESULTS AND DISCUSSION

In this work, 2-methylbutane, 2,2-dimethylbutane, 2,3-dimethylbutane, 2-methylpentane, 3-methylpentane, *n*-pentane, *n*-hexane, methylcyclopentane, and methylcyclohexane were used to synthesize sH hydrate samples with methane gas and to perform solid-state ^{13}C NMR spectroscopic measurements. The ^{13}C NMR spectra of the hydrate samples were compared with those of the pure liquid guests to examine changes in chemical shifts after hydrate formation. The hydrocarbons of this work can be categorized as branched-chain hydrocarbons, branched-cyclic hydrocarbons, and long-chain hydrocarbons, and their isotropic chemical shifts in the pure state at 273.0 K and in the hydrate phase are given in Table 1.

Powder X-ray diffraction (PXRD) was used to identify the structures formed and to obtain lattice parameters, and the corresponding unit cell volumes are presented in Table 2. From the PXRD measurements, the *a* and *c* lattice parameters for the alkane guests vary within the range of 0.1 and 0.013 Å, respectively. The unit cell volumes range between 1289.85 and 1311.75 $Å^3$ for this class of guest molecules and distortions primarily occur in the *a*-direction of the unit cell. The ranges of variation for the lattice parameters are consistent with those of other sH hydrates with nonalkane guests determined by PXRD[22] and molecular dynamics simulations.[23]

Table 1. Experimentally Measured Chemical Shifts of Hydrate Formers in their Pure Form and Hydrate Phases[a]

hydrate formers	carbon label	$\delta_{pure,expt.}$ (ppm)	$\delta_{hydrate}$ (ppm)	$\delta_{pure}-\delta_{hydrate}$ (ppm)
2-methylbutane $(C_\delta H_3)_2C_\gamma HC_\beta H_2C_\alpha H_3$	C_α	12.84	11.56	1.28
	C_δ	22.88 (10.04)	22.39 (10.8)	0.49
	C_γ	30.67 (17.83)	30.67 (19.1)	0.00
	C_β	32.33 (19.49)	32.43 (20.9)	−0.10
2-methylpentane $(C_\varepsilon H_3)_2C_\delta HC_\gamma H_2C_\beta H_2C_\alpha H_3$	C_α	15.18	12.93	2.25
	C_β	21.71 (6.53)	19.36 (6.43)	2.35
	C_ε	23.27 (8.09)	22.92 (9.99)	0.35
	C_δ	28.92 (13.74)	25.10 (12.17)	3.82
	C_γ	42.16 (26.98)	42.16 (29.23)	0.00
3-methylpentane $C_\alpha H_3C_\beta H_2C_\gamma H(C_\delta H_3)C_\beta H_2C_\alpha H_3$	C_α	11.87	11.77	0.10
	C_δ	18.88 (7.01)	17.62 (5.85)	1.26
	C_β	29.79 (17.92)	30.18 (18.41)	−0.39
	C_γ	36.81 (24.94)	36.90 (25.13)	−0.09
2,2-dimethylbutane $(C_\delta H_3)_3C_\gamma C_\beta H_2C_\alpha H_3$	C_α	9.63	8.53	1.10
	C_δ	29.50 (19.87)	29.21 (20.7)	0.29
	C_γ	31.06 (21.43)	30.18 (21.6)	0.88
	C_β	36.90 (27.27)	36.90 (28.4)	0.00
2,3-dimethylbutane $(C_\alpha H_3)_2C_\beta HC_\beta H(C_\alpha H_3)_2$	C_α	20.05	19.08	0.97
	C_β	34.37 (14.32)	34.00 (14.92)	0.37
n-pentane $C_\alpha H_3C_\beta H_2C_\gamma H_2C_\beta H_2C_\alpha H_3$	C_α	14.89	13.72	1.17
	C_β	23.95 (9.06)	21.61 (7.89)	2.34
	C_γ	35.54 (20.65)	34.47 (20.75)	1.07
n-hexane $C_\alpha H_3C_\beta H_2C_\gamma H_2C_\gamma H_2C_\beta H_2C_\alpha H_3$	C_α	14.11	13.24	0.87
	C_β	23.22 (9.11)	20.83 (7.59)	2.39
	C_γ	32.28 (18.17)	28.14 (14.90)	4.14
methylcyclopentane $C_\alpha H_3$-$(C_\beta H(C_\gamma H_2C_\delta H_2)_2)$	C_α	20.93	20.25	0.68
	C_δ	25.80 (4.87)	25.61 (5.36)	0.19
	C_β	35.44 (14.51)	35.44 (15.19)	0.00
	C_γ	35.93 (15.00)	35.93 (15.68)	0.00
methylcyclohexane $C_\alpha H_3$-$(C_\beta H(C_\gamma H_2C_\delta H_2)_2C_\varepsilon H_2)$	C_α	23.95	23.65	0.30
	C_ε	27.36 (3.41)	26.97 (3.32)	0.39
	C_δ	27.36 (3.41)	26.97 (3.32)	0.39
	C_β	33.69 (9.74)	33.71 (10.06)	−0.02
	C_γ	36.12 (12.17)	36.10 (12.45)	0.02

[a] The differences between the chemical shift of the α-carbon and other carbons in each molecule are given in parentheses.

Table 2. Lattice Parameters and Corresponding Unit Cell Volumes of Synthesized Hydrate Samples at 85 K

	lattice parameters/Å		
hydrate formers	*a*	*c*	unit cell volumes/Å^3
2-methylbutane	12.1894	10.0811	1297.19
2-methylpentane	12.2003	10.0709	1298.20
3-methylpentane	12.2241	10.0721	1303.42
2,2-dimethylbutane	12.2664	10.0667	1311.75
2,3-dimethylbutane	12.2541	10.0803	1310.89
n-pentane/2,2 dimethylbutane	12.1597	10.0731	1289.85
n-hexane/2,2 dimethylbutane	12.2667	10.0754	1312.96
methylcyclopentane	12.2011	10.0772	1299.18
methylcyclohexane	12.2014	10.0831	1300.00

Most ^{13}C NMR spectra for the samples show a decrease in chemical shifts (shielding effect) after hydrate formation with changes in chemical shifts found to vary from +0.4 ppm to roughly −4.1 ppm for different guests atoms. Figure 1 shows ^{13}C NMR spectra of 2-methylbutane, 2-methylpentane, and 3-methylpentane. For 2-methylbutane ($(C_\delta H_3)_2C_\gamma HC_\beta H_2C_\alpha H_3$), because the molecule is small enough to be captured into the sH large cages, it was thought to have the same anti conformation as in its pure state. However, it may change its conformation into a gauche-form so that the shielding of the terminal $-C_\alpha H_3$ and $-C_\delta H_3$ atoms is significantly increased. Such an upfield shift is also observed for 2-methylpentane ($(C_\varepsilon H_3)_2C_\delta HC_\gamma H_2C_\beta H_2$-$C_\alpha H_3$), having one more carbon atom than 2-methylbutane. Its conformational change due to the larger molecular size affects the central carbon ($-C_\delta H-$) atom most, while peaks from the terminal $-C_\alpha H_3$ and adjacent $-C_\beta H_2-$ also show significant shielding. However, in the chemical shifts of 3-methylpentane ($C_\alpha H_3C_\beta H_2C_\gamma H(C_\delta H_3)C_\beta H_2C_\alpha H_3$), the branched $-C_\delta H_3$ atom shows the largest shielding effect, while peaks of $-C_\beta H_2-$ atoms in the chain contrarily show the deshielding effect with a downfield shift.

Figure 2 illustrates ^{13}C NMR spectra of 2,2-dimethylbutane and 2,3-dimethylbutane. In the case of 2,2-dimethylbutane

dx.doi.org/10.1021/jp1118184 |J. Phys. Chem. A 2011, 115, 1650–1657

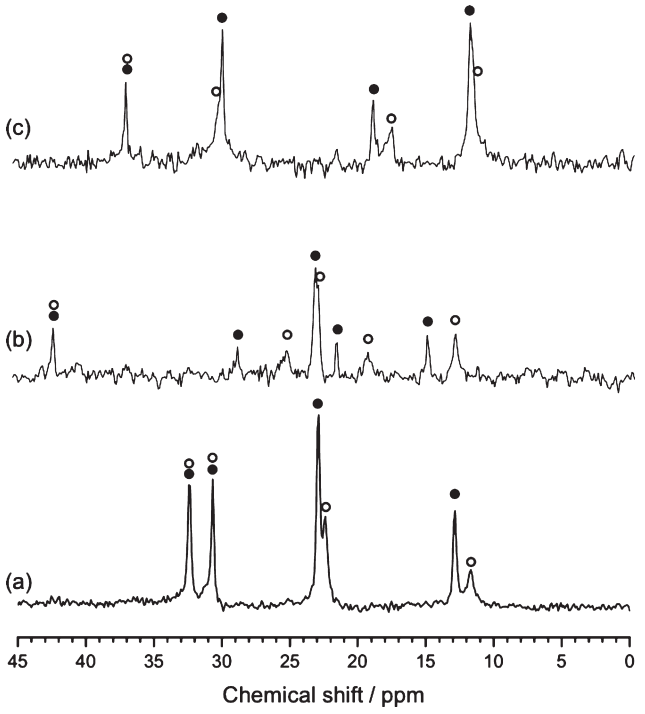

Figure 1. ^{13}C NMR spectra of (a) 2-methylbutane, (b) 2-methylpentane and (c) 3-methylpentane hydrate samples. Filled circles indicate chemical shifts of pure chemicals, while blank circles represent their chemical shifts after hydrate formation.

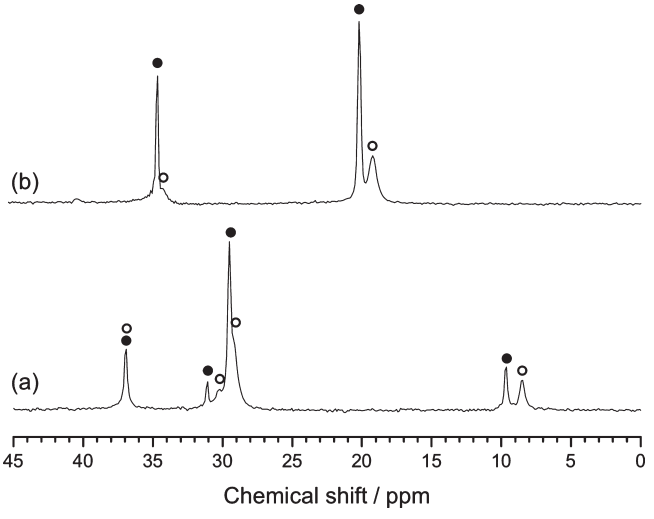

Figure 2. ^{13}C NMR spectra of (a) 2,2-dimethylbutane and (b) 2,3-dimethylbutane hydrate samples. Filled circles indicate chemical shifts of pure chemicals, while blank circles represent their chemical shifts in the hydrate phase.

$((C_\delta H_3)_3C_\gamma C_\beta H_2 C_\alpha H_3)$, changes in the chemical shifts are mainly observed for the terminal $-C_\alpha H_3$ and central $-C_\gamma-$ atoms, whereas the other terminal $-C_\delta H_3$ atoms are also affected. All of the carbon atoms except for $-C_\beta H_2-$ show an upfield shift. For 2,3-dimethylbutane $((C_\alpha H_3)_2 C_\beta H C_\beta H (C_\alpha H_3)_2)$, the terminal $-C_\alpha H_3$ shows significant shielding, while the internal $-C_\beta H-$ atom is also slightly affected.

Figure 3 shows ^{13}C NMR spectra of *n*-pentane and *n*-hexane. As reported in previous literature,[17] these chemicals, formerly known as nonhydrate formers, can participate in the hydrate formation when used as mixtures with other hydrate formers like 2,2-dimethylbutane. They were considered to be nonhydrate formers based on experiments to form sH hydrate with the *n*-alkanes as the only large-cage guest present. Since the length of the all-trans molecules may be a factor in making them nonhydrate formers, their conformations are likely changed to the gauche-form in order to reduce their overall length so as to fit into the hydrate cages.[17]

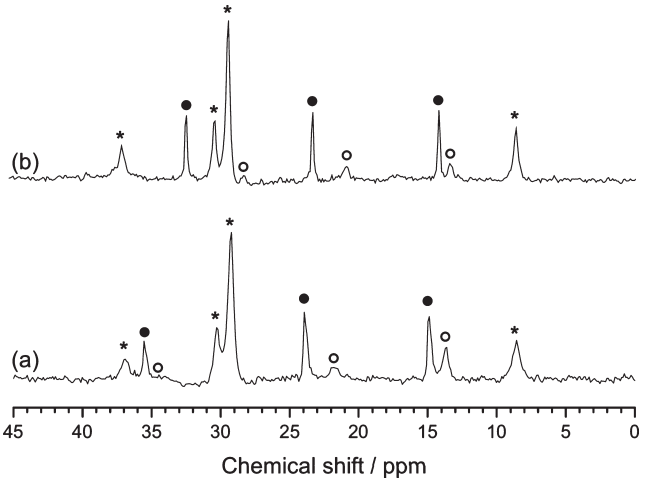

Figure 3. ^{13}C NMR spectra of (a) *n*-pentane and (b) *n*-hexane in both pure and hydrate phases. In this case, another hydrate former, 2,2-dimethylbutane, is used to form mixed hydrates with coguests of *n*-pentane and *n*-hexane. Filled and blank circles indicate chemical shifts of *n*-pentane and *n*-hexane in pure chemical and hydrate phases, respectively, while asterisk marks show chemical shifts from 2,2-dimethylbutane.

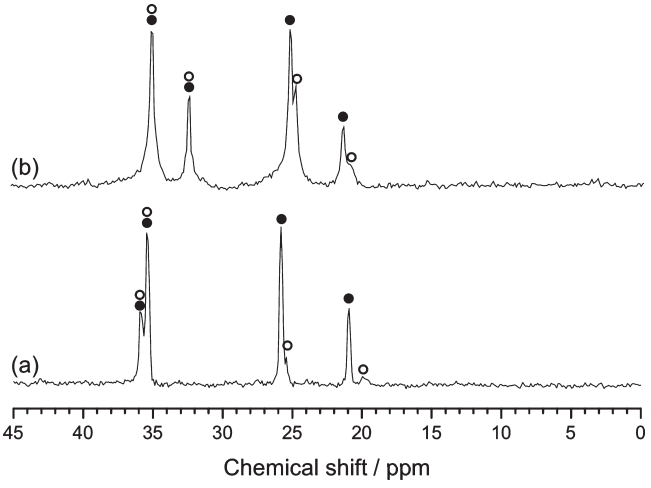

Figure 4. ^{13}C NMR spectra of methyl-substituted cyclic hydrocarbons in both pure and hydrate phases. In these measurements, (a) methylcyclopentane and (b) methylcyclohexane are used.

Finally, ^{13}C NMR spectra of two methyl-substituted cyclic hydrocarbons are provided in Figure 4. As shown by the cyclic hydrocarbons forming sII hydrate, the cyclic sH formers are also only slightly affected due to their structural symmetry and rigidity. However, substituted methyl carbons show significant upfield shifts, while the carbon atoms in the cyclic ring furthest from the substituted methyl group also show a slight upfield shift.

Table 3. Calculated Chemical Shifts of Pure Guest Molecules in Conformations Specified in Table S1 of the Supporting Information

hydrate formers	carbon label	conformer 1	conformer 2	conformer 3	conformer 4
2-methylbutane $(C_\delta H_3)_2C_\gamma HC_\beta H_2C_\alpha H_3$	C_α	9.7	4.3	NA	NA
	C_δ	18.2 (8.4)	16.0 (11.8)		
	C_γ	25.4 (15.2)	23.5 (19.2)		
	C_β	27.1 (17.4)	25.3 (21.0)		
2-methylpentane $(C_\varepsilon H_3)_2C_\delta HC_\gamma H_2C_\beta H_2C_\alpha H_3$	C_α	12.3	12.2	9.5	13.31
	C_β	18.9 (6.6)	12.7 (0.5)	16.2 (6.7)	18.23 (4.92)
	C_ε	18.5 (6.3)	16.6 (4.4)	17.9 (8.4)	18.81 (5.50)
	C_δ	25.2 (12.9)	23.5 (11.2)	20.2 (10.7)	27.41(14.10)
	C_γ	35.6 (23.3)	33.5 (21.3)	33.3 (23.8)	32.25 (18.9)
3-methylpentane $C_\alpha H_3C_\beta H_2C_\gamma H(C_\delta H_3)C_\beta H_2C_\alpha H_3$	C_α	9.9	9.9	6.69	
	C_δ	12.1 (2.1)	16.5 (6.6)	16.51 (9.82)	
	C_β	27.5 (17.6)	24.8 (14.9)	21.10(14.41)	
	C_γ	31.6 (21.6)	31.5 (21.6)	28.74(22.06)	
2,2-dimethylbutane $(C_\delta H_3)_3C_\gamma C_\beta H_2C_\alpha H_3$	C_α	6.6	NA	NA	NA
	C_δ	23.7 (17.1)			
	C_γ	24.9 (18.4)			
	C_β	31.3 (24.7)			
2,3-dimethylbutane $(C_\alpha H_3)_2C_\beta HC_\beta H(C_\alpha H_3)_2$	C_α	17.5	14.6	–	
	C_β	30.2 (12.7)	28.5 (13.9)		
n-pentane $C_\alpha H_3C_\beta H_2C_\gamma H_2C_\beta H_2C_\alpha H_3$	C_α	8.6	7.4	4.8	9.3
	C_β	20.0 (11.4)	17.5 (10.1)	12.8 (8.0)	22.7 (13.4)
	C_γ	31.0 (22.4)	28.6 (21.2)	25.9 (21.0)	25.7 (16.4)
n-hexane $C_\alpha H_3C_\beta H_2C_\gamma H_2C_\gamma H_2C_\beta H_2C_\alpha H_3$	C_α	12.2	11.2	10.7	
	C_β	21.4 (9.2)	20.6 (9.4)	16.9 (6.2)	
	C_γ	29.4 (17.2)	26.9 (15.7)	24.4 (13.8)	
methylcyclopentane $C_\alpha H_3$-$(C_\beta H(C_\gamma H_2C_\delta H_2)_2)$	C_α	12.7	12.3	NA	NA
	C_δ	18.8 (6.1)	16.4 (4.1)		
	C_β	33.7 (21.0)	31.9 (19.6)		
	C_γ	31.0 (18.4)	28.6 (4.1)		
methylcyclohexane $C_\alpha H_3$-$(C_\beta H(C_\gamma H_2C_\delta H_2)_2C_\varepsilon H_2)$	C_α	19.4	14.14	NA	NA
	C_ε	22.1 (2.7)	22.50		
	C_δ	22.5 (3.1)	17.26		
	C_β	27.5 (8.1)	23.70		
	C_γ	29.7 (10.3)	26.59		

The conformers for the guest molecules of Figures 1−4 are shown in Figures S1−S6 of the Supporting Information. Labels and symmetry numbers of each of these conformers are given in Table S1. The relative energies of the conformers, Boltzmann probabilities, $p_i = \exp(-\Delta E_i/RT)\Sigma p_i$, and the longest C···C lengths as a measure of the effective conformer diameter are given in Table S2 of the Supporting Information.

The calculated chemical shifts for all conformers are given in Table 3. Calculated chemical shifts are for the guests in the isolated gas phase but experimental values are for the guests in neat liquid form. To compare the calculated chemical shifts with the experimental liquid-state chemical shifts, Boltzmann-averaged chemical shifts of all calculated conformers should be determined. Calculated chemical shifts are systematically lower than experimental values which is partly related to the known systematic deviations in computed chemical shifts when using the TMS reference.[24] This is usually corrected by applying a regression of the form, $\delta(\text{predicted}) = a + b\delta_{\text{calc.}}$ to improve the agreement between predicted and experimental chemical shifts. The slope factor of $b = 1.1$ is usually applied to calculations of Hartree−Fock and DFT calculated chemical shifts at different levels of theory. As the experimental chemical shifts for the liquid hydrocarbons arise from mixtures of conformers, we have not applied a linear least-squares regression to optimize the agreement between experimental and calculated chemical shifts which represent fixed conformations. To better compare experimental and calculated chemical shifts within each molecule in the liquid state, the differences between the ^{13}C chemical shifts of the α-carbons and the other carbons, $\Delta\delta = \delta(x\text{-carbon}) - \delta(\alpha\text{-carbon})$, with $x = \beta$, γ, δ, or ε are given in Tables 1 and 3. The calculated difference values, $\Delta\delta_{\text{calc.}}$, are easier to compare with the experimental values, $\Delta\delta_{\text{expt.}}$, and are used for analysis. In most cases, the relative order of calculated chemical shifts for the different carbons for each hydrocarbon are in qualitative agreement with the experimental shifts for the pure liquids.

In the sII large cages, X-ray structural analysis has shown that *n*-butane guests have gauche conformations and tetrahydropyran molecules have boat conformations.[25,26] However, X-ray structural analysis of the sH hydrate with 2,2-dimethylpentane guests

dx.doi.org/10.1021/jp1118184 |*J. Phys. Chem. A* 2011, 115, 1650–1657

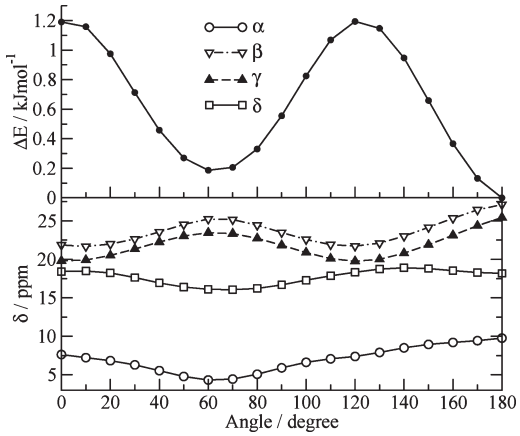

Figure 5. Changes in the chemical shifts of the carbon atoms in 2,2-dimethylbutane and the relative energies with rotation about the 1−4 dihedral angle.

in the large cages shows that this guest is closer to the anti configuration with some deviation from ideal 180° angles.[27] The structural optimization at the B3LYP/6-311++G(*d*,*p*) level shows that the energy difference between the anti and gauche conformers of 2,2-dimethylpentane is high (10.65 kJ·mol^{-1}) and this may lead to unfavorable gauche conformations for this guest. The other alkane guests in this work have much lower minimum dihedral rotation barriers (between 3.5 to 4.1 kJ·mol^{-1}, see Table S2 of the Supporting Information) and gauche conformations may be accessible to the enclathrated molecules. The long axis of the 2,2-dimethylpentane molecule lies parallel to the *z*-axis of the sH unit cell and the long axis of the sH large cage.[27]

For 2-methylbutane, the Boltzmann probabilities given in Table S2 of the Supporting Information suggest that the liquid phase is primarily in the anti conformer (1) of Figure S1 of the Supporting Information. If the $\Delta\delta_{calc.}$ values for the anti conformer (1) are scaled by the factor of 1.1, then the agreement with $\Delta\delta_{expt.}$ is satisfactory. In the hydrate phase, $\delta_{hydrate}$ values for the guest change by 1.28 ppm for the α-carbon, 0.5 ppm for the β-carbon and by smaller amounts for the other two carbons. The calculated values given in Table 3 indicate that these changes in chemical shift are not consistent with the gauche conformer for 2-methylbutane.

The changes in the chemical shifts of the carbon atoms in 2-dimethylbutane with rotation about the 1−4 dihedral angle are shown in Figure 5. The energies corresponding to each dihedral angle are also shown. At room temperature, dihedral angles up to 20° may be accessed for which the chemical shift of the α-carbon, varies within 0.5 ppm, the chemical shifts of the β- and γ-carbons vary up to 2 ppm and the chemical shift of the δ-carbon varies within 0.3 ppm. This pattern of change in chemical shifts does not correspond to the nature of the changes of the experimental chemical shifts of Table 1. We conclude that the changes in chemical shift seen in the hydrate phase, compared to the pure liquid are compatible with interaction effects between the guest and water. This is reasonable since the largest changes in the chemical shifts upon enclathration of the 2-methylbutane guests are for the outermost α- and δ-carbons of the molecule which will interact the most strongly with the cage water molecules.

For 2,3-dimethylbutane, the changes in chemical shift of the α- and β-carbons with the 1−4 dihedral angle are shown in Figure S7 of the Supporting Information. Dihedral angles within 30° of the anti conformation will be energetically accessible and the chemical shift variation in this range is up to 0.2 and 2.5 ppm for the α- and β-carbons, respectively. The changes in experimental chemical shift upon enclathration for the α- and β-carbons are 0.97 and 0.37 ppm, respectively, which are incompatible with both the small changes in the dihedral angle about the anti conformation (discussed above) and the gauche 2,3-dimethylbutane conformation chemical shifts given in Table 3. Once again, we can conclude that the change in chemical shifts is due primarily to the interactions of the 2,3-dimethylbutane guest carbon atoms which, as expected, is greater in magnitude for the outermost α-carbons.

For the 2,2-dimethylbutane guest, the changes in chemical shift as a function of the 1−4 dihedral angle are shown in Figure S8 of the Supporting Information. Dihedral angle variations up to 35° may be accessed at 273.0 K. Within this range of dihedral angle, the chemical shifts of the α-, β-, γ-, and δ- carbons change by ∼0.9, 1.9, 0.9, and 0.7 ppm. This molecule has no gauche conformation. Given the pattern of the changes in experimental chemical shifts upon enclathration for the α-, β-, γ-, and δ- carbons, which from Table 1 are 1.10, 0.29, 0.84, and 0.00 ppm, respectively, we conclude that the changes in chemical shifts between the pure liquid and hydrate phase are incompatible with only small changes in the dihedral angle about the anti conformation and that changes in chemical shifts are primarily due to the interactions of the 2,2-dimethylbutane guest α- and γ-carbon atoms with the cage waters.

Of the other guests studied in this work, *n*-pentane, 2-methylpentane, and 3-methylpentane have five carbon chains. Experimental X-ray structural analysis on 2,2-dimethylpentane[27] shows that the five carbon chain is in the all anti conformation, with some deviation from the ideal 180° angles. For the three pentane-based guests of this work, the conformation space is more complex and consists of two dihedral angles. To characterize this dihedral angle/energy/chemical shift space, we would need to make a Ramachandran-like plot for the conformers. Given the computational time required, we have not attempted to prepare these plots and limit the discussion to qualitative arguments for these guests.

For 2-methylpentane, the $\Delta\delta_{calc.}$ values for the all anti conformation in Table 3 are the most compatible with the experimental $\Delta\delta_{expt.}$ for the pure liquid given in Table 1. However, significant deviations from the ideal 180° angle may be expected for the $C_\alpha-C_\beta-C_\gamma-C_\delta$ dihedral angle. According to the Boltzmann probabilities given in Table S2 of the Supporting Information, some contribution from the low energy "α-gauche ε-anti" (3) conformation may also be expected. In the hydrate form, the $\Delta\delta_{calc.}$ values agree well with the (α-gauche ε-anti) conformation as well. The large experimentally observed changes in the chemical shifts for the interior β- and δ-carbons suggest that a conformational change has occurred upon enclathration of this guest. The large change in chemical shift for the α-carbon between the pure liquid and hydrate can also be partially explained by the change in conformation from the all anti conformation to the (α-gauche ε-anti) conformation.

For 3-methylpentane, the $\Delta\delta_{calc.}$ values for the all anti and low-energy antigauche (2) (see Figure S3 of the Supporting Information) conformations in Table 3 are the most compatible with the experimental $\Delta\delta_{expt.}$ for the pure liquid given in Table 1. In the hydrate form, the experimental $\Delta\delta_{expt.}$ is also compatible with a mixture of these two conformers, but with different composition. The largest change in chemical shift with hydrate formation is for the δ-carbon (1.26 ppm). This change is

compatible with the large difference for the chemical shift of this carbon between the all anti and anti-gauche (2) conformation, but can also be due to the interactions of this carbon with the cage waters. The δ-carbon protrudes out of the five carbon backbone and may interact strongly with cage waters. The chemical shift difference between the pure liquid and hydrate for the exposed α-carbons is small (0.1 ppm).

For *n*-pentane, the experimental $\Delta\delta_{expt.}$ Values for the pure liquid given in Table 1 are most compatible with the $\Delta\delta_{calc.}$ values for the relatively high energy gauche−gauche (2) conformation in Table 3. However, the Boltzmann probability would predict that this conformer is only constitutes up to 6% of the *n*-pentane mixture (see Table S2 of the Supporting Information). However, the poor solubility of *n*-pentane in water may affect the distribution of conformations for the pure liquid that gives rise to the results of Table 1 and Figure 3. The changes in chemical shift on hydrate formation for the α-, β-, and γ-carbons in *n*-pentane are large (1.17, 2.34, and 1.07 ppm, respectively). The large changes in the chemical shifts of the interior β- and γ-carbons imply large dihedral angle changes in this molecule during hydrate formation. The conformational state of *n*-hexane is similarly unclear. However, very large changes in the chemical shift for the β- and γ-carbons upon hydrate formation (2.39 and 4.14 ppm, respectively, see Table 1) imply there are large conformational changes to this molecule on hydrate formation.

For methylcyclopentane the largest chemical shift change upon hydrate formation (0.68 ppm) is related to the α-carbon which shows there is likely not much conformational change in this relatively rigid molecule upon hydrate formation. The qualitative differences between the $\Delta\delta_{expt.}$ for the pure liquid given in Table 1 and the $\Delta\delta_{calc.}$ values for the equatorial conformer in Table 3 show there are deviations from the ideal gas phase dihedral angles in both the pure liquid phase and the hydrate.

For methylcyclohexane the chemical shift changes upon hydrate formation for the carbons are relatively small and equivalent to 0.3, 0.39, and 0.39 ppm for the α-, ε-, and δ-carbons, respectively. These changes in chemical shift occur on the most exposed carbons and are likely due to interactions with the cage walls. The observed $\Delta\delta_{expt.}$ values for the pure liquid given in Table 1 are in good agreement with the $\Delta\delta_{calc.}$ values for the equatorial conformer in Table 3. X-ray crystal structure analysis is available for the methylcyclohexane binary sH hydrate with methane help gas.[24] The methylcyclohexane molecule is in the chair conformation with the long axis pointing in the direction of the *z*-axis of the unit cell. This allows the long axis of the molecule to be accommodated along the long axis of the large sH cage to minimize guest-cage repulsions. This also explains the relatively small changes in guest chemical shifts upon hydrate formation.

To explicitly calculate the effect of the cage on the ^{13}C chemical shifts, we would need to calculate the chemical shielding of the guests in positions in the cage determined by X-ray crystal structure analysis. Computational optimization of the guest positions in clathrate hydrates, which are determined by repulsive packing and nonbonding interactions between the guest and the cage wall, is difficult to perform and guest positions determined in this manner are presently not reliable. The present calculations thus do not unambiguously determine the relative contributions of conformational changes and cage wall-guest interactions in changing the guest ^{13}C NMR chemical shifts. However, they can contribute to deconvoluting these two effects and until such time as the positions of the molecules in the cages are crystallographically determined, this analysis can be helpful in determining guest shapes and strengths of coupling in the cages.

The effect of the hydrate cage water molecules on the ^{13}C chemical shift of methane in small and large cages of sI and sII phases has been studied[11] and a range in chemical shift between −7 ppm for gas phase methane to −2.73 ppm for methane in the small sII small cages is observed. This change in chemical shift is the result of interactions between methane and the cage water molecules and is consistent with the magnitude of changes between the chemical shifts of the free guests and encapsulated guests in the sH hydrate.

CONCLUSIONS

Binary sH hydrates of methane and well-known hydrate formers of 2-methylbutane, 2,2-dimethylbutane, 2,3-dimethylbutane, 2-methylpentane, 3-methylpentane, *n*-pentane, *n*-hexane, methylcyclopentane, and methylcyclohexane were synthesized. These samples were characterized by means of ^{13}C NMR spectroscopic methods, powder X-ray diffraction, and computation. From the X-ray diffraction measurements, the *a* lattice parameter was found to change within a range of 0.1 Å between the different hydrate formers. In the case of the NMR spectra, chemical shifts of the hydrate formers show different peak positions in the hydrate phase from those in the pure chemical states. Computational analysis of the different conformers of the guest molecules allows us to understand possible changes in the guest conformations upon hydrate formation and to estimate the effect of interactions with the cage water molecules on the chemical shifts of the guests. The experimental and computational results obtained in this work are thought to give fundamental information on molecular behaviors of structure H guests during hydrate formation.

ASSOCIATED CONTENT

Supporting Information. The conformers for the guest molecules of Figures 1−4 (Figures S1−S6; labels and symmetry numbers of each of these conformers (Table S1); the longest C···C lengths as a measure of the effective conformer diameter (Table S2); the changes in chemical shift of the α- and β-carbons with the 1−4 dihedral angle of 2,3-dimethylbutane (Figure S7); and the changes in chemical shift as a function of the 1−4 dihedral angle of the 2,2-dimethylbutane guest (Figure S8). This material is available free of charge via the Internet at http://pubs.acs.org.

AUTHOR INFORMATION

Corresponding Author

*Tel: + 1-613-993-2011. Fax: +1-613-998-7833. E-mail: john.ripmeester@nrc.ca.

REFERENCES

(1) Sloan, E. D. Clathrate *Hydrates of Natural Gases*, 2nd ed.; Marcel Dekker, Inc.: New York, 1998.

(2) Wilcox, W. I.; Carson, D. B.; Katz, D. L. *Ind. Eng. Chem.* **1941**, *33*, 662.

(3) Kang, S.-P.; Chun, M. K.; Lee, H. *Fluid Phase Equilib.* **1998**, *147*, 229.

(4) Eichholz, C.; Majumdar, A.; Clarke, M. A.; Oellrich, L. R.; Bishnoi, P. R. *J. Chem. Eng. Data* **2004**, *49*, 847.

(5) Seo, Y.-T.; Moudrakovski, I. L.; Ripmeester, J. A.; Lee, J.-W.; Lee, H. *Environ. Sci. Technol.* **2005**, *39*, 2315.
(6) Kang, S.-P.; Lee, H. *Environ. Sci. Technol.* **2000**, *34*, 4397.
(7) Gudmundsson, J. S.; Parlaktuna, M.; Khokhar, A. A. *Soc. Petrol. Eng. Prod. Facil.* **1994**, *9*, 69.
(8) Sum, A. K.; Burruss, R. C.; Sloan, E. D. *J. Phys. Chem. B* **1997**, *101*, 7371.
(9) Choi, Y. N.; Yeon, S.-H.; Park, Y.; Choi, S.; Lee, H. *J. Am. Chem. Soc.* **2007**, *129*, 2208.
(10) Davidson, D. W.; Handa, Y. P.; Ripmeester, J. A. *J. Phys. Chem.* **1986**, *90*, 6549.
(11) Ripmeester, J. A.; Ratcliffe, C. I. *J. Phys. Chem.* **1988**, *92*, 337.
(12) Collins, M. J.; Ratcliffe, C. I.; Ripmeester, J. A. *J. Phys. Chem.* **1990**, *94*, 157.
(13) Kim, D.-Y.; Lee, H. *J. Am. Chem. Soc.* **2005**, *127*, 9996.
(14) Ripmeester, J. A.; Ratcliffe, C. I. *J. Phys. Chem.* **1990**, *94*, 8773.
(15) Ratcliffe, C. I. *Annu. Rep. NMR Spectrosc.* **1998**, *36*, 123.
(16) Moudrakovski, I. L.; Sanchez, A. A.; Ratcliffe, C. I.; Ripmeester, J. A. *J. Phys. Chem. B* **2001**, *105*, 12338.
(17) Lee, J.-W.; Lu, H.; Moudrakovski, I. L.; Ratcliffe, C. I.; Ripmeester, J. A. *Angew. Chem., Int. Ed.* **2006**, *45*, 2456.
(18) Kim, D. Y.; Uhm, T. W.; Lee, H.; Lee, Y. J.; Ryu, B. J.; Kim, J. H. *Korean J. Chem. Eng.* **2005**, *22*, 569.
(19) Lu, H.; Seo, Y.-T.; Lee, J.-W.; Moudrakovski, I. L.; Ripmeester, J. A.; Chapman, N. R.; Coffin, R. B.; Gardner, G.; Pohlman, J. *Nature* **2007**, *445*, 303.
(20) (a) Wolinski, K.; Hinton, J. F.; Pulay, P. *J. Am. Chem. Soc.* **1990**, *112*, 8251. (b) Rauhut, G.; Puyear, S.; Wolinski, K.; Pulay, P. *J. Phys. Chem.* **1996**, *100*, 6310–6316. (c) Cheeseman, J. R.; Trucks, G. W.; Keith, T. A.; Frisch, M. J. *J. Chem. Phys.* **1996**, *104*, 5497.
(21) Frisch, M. J.; Trucks, G. W.; Schlegel, H. B.; Scuseria, G. E.; Robb, M. A.; Cheeseman, J. R.; Zakrzewski, V. G.; Montgomery, J. A., Jr.; Stratmann, R. E.; Burant, J. C.; Dapprich, S.; Millam, J. M.; Daniels, A. D.; Kudin, K. N.; Strain, M. C.; Farkas, O.; Tomasi, J.; Barone, V.; Cossi, M.; Cammi, R.; Mennucci, B.; Pomelli, C.; Adamo, C.; Clifford, S.; Ochterski, J.; Petersson, G. A.; Ayala, P. Y.; Cui, Q.; Morokuma, K.; Malick, D. K.; Rabuck, A. D.; Raghavachari, K.; Foresman, J. B.; Cioslowski, J.; Ortiz, J. V.; Stefanov, B. B.; Liu, G.; Liashenko, A.; Piskorz, P.; Komaromi, I.; Gomperts, R.; Martin, R. L.; Fox, D. J.; Keith, T.; Al-Laham, M. A.; Peng, C. Y.; Nanayakkara, A.; Gonzalez, C.; Challacombe, M.; Gill, P. M. W.; Johnson, B. G.; Chen, W.; Wong, M. W.; Andres, J. L.; Head-Gordon, M.; Replogle, E. S.; Pople, J. A. GAUSSIAN 98 (Revision A.7), Gaussian Inc., Pittsburgh, PA, 2001.
(22) Takeya, S.; Hori, A.; Uchida, T.; Ohmura, R. *J. Phys. Chem. B* **2006**, *110*, 12943.
(23) Miyoshi, T.; Ohmura, R.; Yasuoka, K. *Mol. Simul.* **2007**, *33*, 65.
(24) (a) Baldrigde, K. K.; Siegel, J. S. J. *Phys. Chem. A* **1999**, *103*, 4038. (b) Barone, G.; Duca, D.; Silvestri, A.; Gomez-Paloma, L.; Riccio, R.; Bifulco, G. *Chem.—Eur. J.* **2002**, *8*, 3240. (c) Auer, A. A.; Gauss, J.; Stanton, J. F. *J. Chem. Phys.* **2003**, *118*, 10407.
(25) Davidson, D. W.; Garg, S. K.; Gough, S. R.; Hawkins, R. E.; Ripmeester, J. A. *Can. J. Chem.* **1977**, *55*, 3641.
(26) Udachin, K. A.; Ratcliffe, C. I.; Ripmeester, J. A. *J. Supramol. Chem.* **2002**, *2*, 405.
(27) Udachin, K. A.; Ratcliffe, C. I.; Enright, G. D.; Ripmeester, J. A. *Supramol. Chem.* **1997**, *8*, 173.